

The double-temperature ratchet model and current reversal of coupled Brownian motors

Chen-Pu Li,^{1,2} Hong-Bin Chen,^{3,4} and Zhi-Gang Zheng^{3,4,*}

¹ *Department of Physics, Beijing Normal University, Beijing 100875, China*

² *College of Science, Hebei University of Architecture, Zhang Jiakou 075000, China*

³ *Institute of Systems Science (ISS), Huaqiao University, Xiamen 361021, China*

⁴ *College of Information Science and Engineering, Huaqiao University, Xiamen 361021, China*

(Dated: October 5, 2016)

Based on the transport features and experimental phenomena observed in studies of molecular motors, we proposed the double-temperature ratchet model of coupled motors to reveal the dynamical mechanism of cooperative transport of motors with two heads, where the interactions and the asynchronous between two motor heads are taken into account. We investigated the collective unidirectional transport of coupled system, and find that the direction of motion can be inverted under certain conditions. Inverse motion can be achieved by modulating the coupling strength, the coupling free length and the asymmetric efficient of the periodic potential, which is understood in terms of the effective-potential theory. The dependence of directed current on various parameters is studied systematically. Directed transport of coupled Brownian motors can be manipulated and optimized by adjusting pulsating period or the phase shift of the pulsating temperature.

PACS numbers: 05.45.Xt, 05.40.-a, 05.60.-k02.50.Ey

I. INTRODUCTION

The directed transport of Brownian motors in periodic structures with the help of fluctuations with zero mean has long been an important problem, which has been widely studied [1–4]. In recent years, people have paid much attention to the theoretical studies of directed transport of coupled Brownian motors in many different scientific backgrounds, such as molecular motors in biological systems, divergence of two polymers on the surface and Josephson junction arrays, to name but a few [5–16]. A non-equilibrium environment and the broken symmetry of the system are indispensable conditions for the directional transport of particles in a ratchet model. In generally, symmetry breaking includes the symmetry breaking of the periodic potential field, the symmetry breaking induced by non-equilibrium perturbations, and the breaking induced by mutual coupling between elements in the system [17–27].

In the present work, we address the case of two interacting Brownian motors in a spatially periodic potential. The motivation of this topic comes from the experimental observations of the motion patterns of molecular motors (protein motors). It was found that most of the protein motors possess the dimer structure that each motor protein is composed of two interacting identical monomers, and each monomer experiences the cyclic ATP hydrolyzing process [28, 29]. It was experimentally found that the coupling between two motor proteins, which do not act independently but alternate in a sequential manner such that their catalytic cycles are out of phase, plays a significant role in achieving directed motion and even

the reversed motion. We noticed an important fact in relating to the symmetry breaking of dimer molecular motors, i.e., it was also found that the hydrolysis processes of two heads are continuous while asynchronous [30, 31]. This gives us a hint for setting up the double-temperature ratchet model of coupled motors in a asymmetric potential field.

In this paper we will analyze the effects of several parameters on the average velocity of coupled motor, such as coupling strength, the asymmetry coefficient of potential, the pulsating period and phase shift of temperature. Otherwise, the dynamical mechanism and reverse behavior of the coupled motor is reasonably explained based on effective potential theory in strong-coupling case.

II. THE COUPLED DOUBLE-TEMPERATURE BROWNIAN MOTOR MODEL

A. Dynamical Model

We consider the over-damped Brownian motion of two coupled Brownian motors contacting with two reservoirs with different temperatures in asymmetric periodic potentials. The equations of motion of two mutually coupled motors can be written as

$$\dot{x}_i = -\frac{\partial V(x_i)}{\partial x_i} - \frac{\partial U_0}{\partial x_i} + \xi_i(t), \quad i = 1, 2 \quad (1)$$

where x_i is the coordinate of the i -th motor, $V(x)$ is the asymmetric periodic potential that is originated from the interaction between the motor and the track, which is chosen as the following simplified form:

$$V(x) = -V_0[\sin(\frac{2\pi}{L}x) + \frac{\Delta}{4}\sin(\frac{4\pi}{L}x)] \quad (2)$$

*zgzheng@hqu.edu.cn.

with L the spatial period of the potential field $V(x)$, which is shown in Fig.1, where Δ is the asymmetry coefficient of the potential field $V(x)$. $U_0(x_1, x_2)$ denotes the interaction potential between two motors, which is set to be the following simple harmonic form:

$$U_0(x_1, x_2) = \frac{1}{2}k(x_1 - x_2 - a)^2, \quad (3)$$

k is the coupling strength, and a is the coupling free length. The influence of two reservoirs to the Brownian motors are described in terms of the noise $\xi_1(t)$ and $\xi_2(t)$, and they are assumed to be independent and unbiased Gaussian white noises with

$$\begin{aligned} \langle \xi_i(t) \rangle &= 0, \\ \langle \xi_i(t) \xi_j(t') \rangle &= 2k_B T_i(t) \delta_{ij} \delta(t - t'), \quad i, j = 1, 2 \end{aligned} \quad (4)$$

where $k_B T$ is the thermal energy, and $T_1(t)$, $T_2(t)$ are the following modulated harmonically varying functions

$$\begin{aligned} T_1(t) &= T_0 [1 + A \sin(\frac{2\pi}{t_0} t)]^2, \\ T_2(t) &= T_0 [1 + A \sin(\frac{2\pi}{t_0} t + \Delta\theta)]^2, \end{aligned} \quad (5)$$

with A the amplitude of temperature, t_0 the pulsating period of temperature, and $\Delta\theta$ is the phase shift between two temperature fluctuations. The mismatch between two different temperatures denotes biologically the different ATP-Hydrolysis states in two motors,

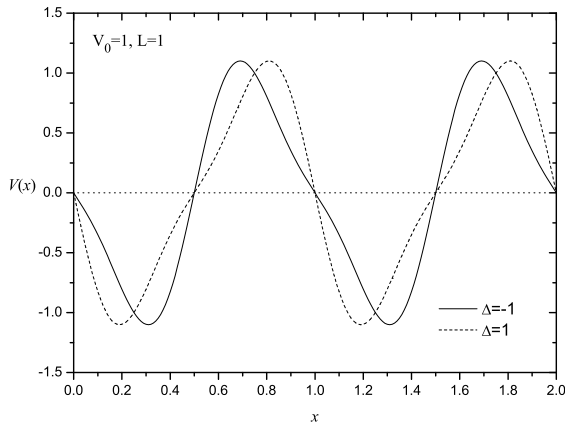


FIG. 1: the asymmetric periodic potential $V(x)$ which is originated from the interaction between the motor and the track.

B. Adiabatic Elimination and Mass-Center Dynamics in Strong-coupling case

It is difficult to directly analyze the cooperative ratcheting effect of two coupled Brownian motors theoretic-

ally. An effective method in dealing with the cooperative ratcheting effect of coupled motors is to decrease the degrees of freedom of the system to get a low-dimensional description. By introducing the mass-center coordinate $X = (x_1 + x_2)/2$ and the relative coordinate $Y = x_1 - x_2$, one can transform Eqs. (1) to

$$\begin{aligned} \dot{X} &= -\frac{1}{2} \frac{\partial [V(X + \frac{Y}{2}) + V(X - \frac{Y}{2})]}{\partial X} \\ &\quad - \frac{\partial [V(X + \frac{Y}{2}) - V(X - \frac{Y}{2})]}{\partial Y} + \frac{1}{2}(\xi_1(t) + \xi_2(t)), \end{aligned} \quad (6)$$

$$\begin{aligned} \dot{Y} &= -\frac{\partial [V(X + \frac{Y}{2}) - V(X - \frac{Y}{2})]}{\partial X} \\ &\quad - 2 \frac{\partial [V(X + \frac{Y}{2}) - V(X - \frac{Y}{2})]}{\partial Y} - 2k(Y - a) + \xi_1(t) - \xi_2(t). \end{aligned} \quad (7)$$

In order to understand the effect of the coupling between two Brownian motors on directed transport of the system, it is instructive to study the dynamics in the limit of large but finite stiffness k . In this situation, the term $-2k(Y - a)$ in Eq.(7) implies a much faster decay of the coordinate Y as compared with the relaxation of the variable X . This analysis indicates that Y is a fast variable and can be adiabatically eliminated in terms of the slaving principle proposed by H. Haken [10, 27, 32]. Therefore in $k \rightarrow \infty$ the dynamical equation of the mass-center of coupled motors can be described as

$$\begin{aligned} \dot{X} &= -\frac{1}{2} \frac{\partial [V(X + \frac{a}{2}) + V(X - \frac{a}{2})]}{\partial X} \\ &\quad + \frac{1}{2}(\xi_1(t) + \xi_2(t)), \end{aligned} \quad (8)$$

with $Y \approx a$.

The dynamical equation (8) can be simply expressed as

$$\dot{X} = f(X) + q(t), \quad (9)$$

with

$$\begin{aligned} f(X) &= -\frac{1}{2} \frac{\partial [V(X + \frac{a}{2}) + V(X - \frac{a}{2})]}{\partial X}, \\ q(t) &= \frac{1}{2}(\xi_1(t) + \xi_2(t)). \end{aligned}$$

Theoretically this enables one to qualitatively calculate the effect of multiple parameters, such as the coupling free length a , the modulation period t_0 of two temperatures, and the phase shift $\Delta\theta$ between two temperatures, on the ratchet motion of the coupled Brownian motors in terms of the dynamics of a single Brownian motor (the mass-center dynamics).

According to the analyses in reference [4] on the temperature ratchet of a single Brownian motor, when the period t_0 of the temperature fluctuation tends to infinity,

the temperature can be regarded as an approximate constant in a small-time interval, where the average velocity of a single Brownian motor is zero in the periodic potential with Gaussian white noise. When the period $t_0 \ll 1$, one can readily find that

$$\langle \dot{X} \rangle = t_0^2 B_k \int_0^L dX (V'_k(X) [V''_k(X)]^2) + o(t^3), \quad (10)$$

with

$$B_k = \frac{4L \int_0^1 dh [\int_0^h d\hat{h} (\frac{1-\hat{T}(\hat{h})}{T})]}{\eta^3 \int_0^L dX (e^{\frac{V_k(X)}{k_B T}}) \int_0^L dX (e^{-\frac{V_k(X)}{k_B T}})}$$

and

$$\bar{T} = \frac{1}{t_0} \int_0^{t_0} dt T(t) = \int_0^1 dh \hat{T}(h),$$

$$\hat{T}(h) = T(t) = T(t_0 h).$$

C. Effective Potential Theory in Strong-coupling case

In order to explain the current reversal of the ratchet system it is convenient to introduce the effective potential [10, 24, 27]. In the above discussion we know that in strong-coupling situation the dynamics of the relative coordinate Y occurs on a much faster time scale than that of the mass-center coordinate X . one can obtain the effective potential $V_{eff}(X)$ of X by replacing the X - and Y -dependent potential with the potential averaged with respect to the fast relative coordinate Y as

$$V_{eff}(X) = -\frac{1}{2} k_B \bar{T} \ln \left(\int_{-\infty}^{\infty} dY \rho(X, Y) \right), \quad (11)$$

and

$$\rho(X, Y) = e^{-\frac{U(X, Y)}{k_B T}}, \quad (12)$$

$$U(X, Y) = \frac{1}{2} k (Y - a)^2 + V(X + \frac{Y}{2}) + V(X - \frac{Y}{2}). \quad (13)$$

In the following discussions we go on studying the collective directed transport of the coupled Brownian motors in terms of numerical simulations and make comparisons with theoretical discussions. In numerical simulations of the stochastic dynamics, the second-order Runge-Kutta numerical simulation algorithm is adopted [33, 34], and the number of ensembles $N=1000$, the time step $dt=0.001$. Throughout numerical simulations we set parameters $V_0=1$ and $L=1$. The average velocity or the current can be obtained by executing both ensemble and time averages on the instantaneous velocity as

$$v = \langle \dot{x} \rangle = \lim_{t \rightarrow \infty} \frac{1}{NT} \sum_{i=1}^N \int_0^t dt' \dot{x}_i(t'). \quad (14)$$

III. COLLECTIVE DIRECTED TRANSPORT AND CURRENT REVERSAL

In this section, we analyze the influence of the coupling coefficient k of the coupled Brownian motors, the coupling free length a and the phase shift $\Delta\theta$ of two motor heads on the average velocity. Theoretically one can discuss the current reversal based on the effective potential theory for strong-coupling case.

A. Current reversal induced by the coupling strength

The coupling strength k plays a significant role on directed transport of the ratchet system. Fig.2(a) gives three curves of the average velocity against the coupling strength k with different phase shifts $\Delta\theta = \pi, \pi/2$, and 0 respectively. Fig.2 (b) presents the curves of the effective potential with different coupling strengths $k=0, k=300$, and $k=1000$ (corresponding to the strong-coupling limit $k \rightarrow \infty$ in theoretical analysis). In Fig.2 (a) every curve has the same feature that the sign of the velocity, corresponding to the direction of motion of the coupled motors, can be reversed when the coupling strength k reaches a certain value.

For the case of weak coupling (e.g., $0.01 < k < 1$ in Fig.2 (a)) the average velocity $v \approx -0.22$. This is because in weak-coupling case the motion can be considered as a simple composition of that of two single motors, where each particle is immersed in a common periodic potential $V(x)$ and the Gaussian white noise, and the effective potential $V_{eff}(X)$ (e.g., the curve with $k=0$ in Fig.2 (b)) of mass center could be considered as the potential $V(x)$ of a single motor, and the motion of two weakly-coupled motors is consistent with the relatively large gradient of the potential $V(x)$ in the temperature ratchet model of single motor [10]. With the increase of the coupling strength k (e.g., $k = 1 \sim 40$ in Fig.2 (a)) the negative mean velocity gradually increases and tends to zero, which shows that the coupling between the two coupled motors affects the symmetry breaking of the whole system. When the coupling is large enough (e.g., $k \sim 40-1000$ in Fig.2 (a)), the symmetry breaking is opposite to that when the coupling is weak ($k \sim 0$ to 40 in Fig.2 (a)), such as the effective potential $V_{eff}(X)$ in strong coupling case exhibits a reversed tendency relative to that of weak coupling case in Fig.2 (b). Finally, the positive mean velocity reaches a saturation with the increase of the coupling strength k .

In addition, in Fig.2 (a) it can be found that when $k < 40$ the three curves almost coincide with each other, and the effects of phase shift $\Delta\theta$ on the average velocity is very small. That is because of the single-particle features and the independence of the mean velocity on $\Delta\theta$ for weak-coupling case. When $k > 40$ the mean velocity decreases as the increase of $\Delta\theta$ in the range of $[0, \pi]$ and tends to zero for $\Delta\theta = \pi$. This can be interpreted in terms of the formulas of the two tempo-

rally modulated temperatures $T_1(t)=T_0[1+\sin(2\pi t/t_0)]^2$ and $T_2(t)=T_0[1+\sin(2\pi t/t_0+\Delta\theta)]^2$. In the temperature ratchet model, the maximum temperature implies a minimum binding of the potential well to the coupled motors, and the minimum temperature corresponds to the strongest binding. According to the two formulas with $\Delta\theta = \pi$, one temperature of the coupled motors reaches the maximum value when the other one is the minimum, that implies that the coupling reduces the motion of coupled motor in this case. For $\Delta\theta = 0$ the temperatures fluctuation at both motors is synchronized, which means that the average velocity reaches the maximum value because the coupling could enhance the motion.

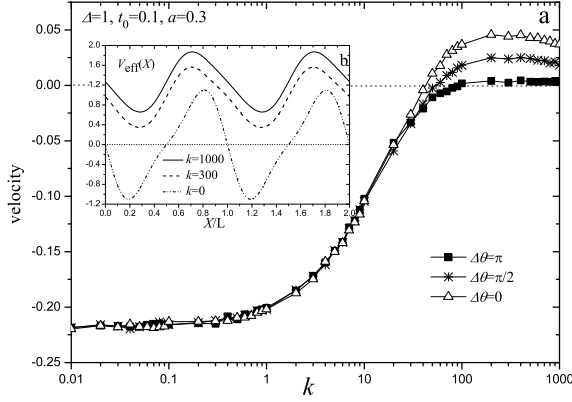


FIG. 2: the mean velocity as a function of the coupling strength k .

B. Current reversal induced by changing the coupling free length

The presence of the coupling between two motor heads not only provides the cooperative directed motion, but also plays a significant role in influencing the current. The direction of the current can even be determined by the free length of the coupled motors, where the current reversal can be well interpreted in terms of the effective potential theory.

In Fig.3(a) we give the average velocity varying against the coupling free length a with other parameters given in the plot, where four curves correspond to different coupling strengths k and different phase shifts $\Delta\theta$ between the two temperatures, i.e., $(k, \Delta\theta) = (1, 0)$, $(300, 0)$, $(300, \pi/2)$, $(300, \pi)$, respectively. It can be found from Fig.4 (a) that when the coupling strength k is small (e.g., $k = 1$) the coupling free length a cannot greatly influence the average velocity which is almost kept a negative constant (e.g., $v = -0.2$) for all the value of a . This is because the motion of coupled motors can be considered as a simple composition of two single motors in weak-

coupling cases. For the three curves with strong coupling strengths k (e.g., $k = 300$) between the two motors in Fig.3 (a), it can be observed that the average velocity first increases and then decreases with a in the range of 0 to $L/2$, and the reversal of velocity occurs when $a = L/4$. In addition, these curves are symmetric about $a = L/2$. In Fig.3 (b), the average velocity versus the coupling free length a is theoretically computed according to Eq.(10) with the parameters given in the plot. Although there are differences from the simulation results in Fig.3 (a), the theoretical results can still qualitatively display the effects of the coupling free length a on the average velocity. Note that only when t_0 is close to zero the theoretical results agree well with that of the simulation.

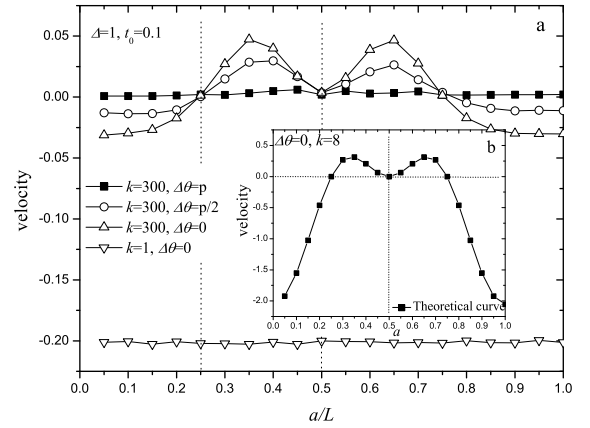


FIG. 3: the mean velocity as function of the coupling free length a .

In Figs.4(a),(b),(c) and (d) we give four curves of the effective potential $V_{eff}(X)$ for the coupling free length $a=0.1, 0.25, 0.3$ and 0.5 respectively, where other parameters $k=300, \Delta=1$. In the strong-coupling case the asymmetric coefficient of the effective potential $V_{eff}(X)$ periodically changes against the coupling free length a with L as one cycle in Fig.4 a,b, c, and d. It can be found from Fig.4 that the asymmetric coefficient $\Delta_{eff} > 0$ when $0 < a < L/4$, $\Delta_{eff} < 0$ when $L/4 < a < L/2$, and $\Delta_{eff} = 0$ when $a = L/4$ and $L/2$. The evolutionary behavior of the average velocity agrees well with the change of the asymmetric coefficient of the effective potential $V_{eff}(X)$ for the strong-coupling situations shown in Fig.4, which naturally leads to the periodic variation of the average velocity.

The symmetry about $a = L/2$ of the average velocity can be well understood through the analysis of the space-time transformation invariance of dynamical Eq. (1) [25, 27, 35, 36]. By rewriting Eq.(1) with a superscript corresponding to the value of coupling free length a as

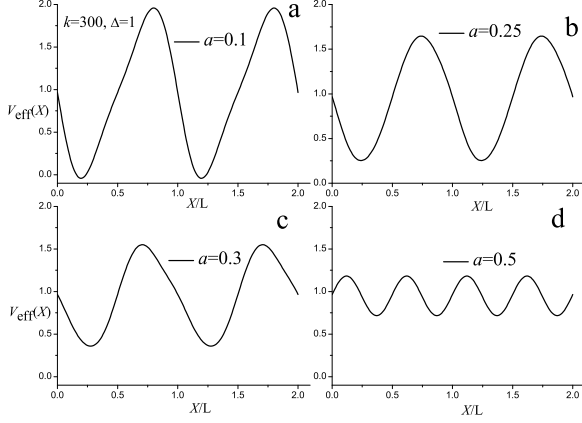


FIG. 4: the curves of effective potential with different the free length a .

$$\begin{aligned}\dot{x}_1^{(a)} &= -\frac{\partial V(x_1)}{\partial x_1} - k(x_1 - x_2 - a) + \xi_1(t), \\ \dot{x}_2^{(a)} &= -\frac{\partial V(x_2)}{\partial x_2} + k(x_1 - x_2 - a) + \xi_2(t).\end{aligned}\quad (15)$$

By replacing the free length a by $L - a$, one obtains

$$\begin{aligned}\dot{x}_1^{(L-a)} &= -\frac{\partial V(x_1)}{\partial x_1} - k(x_1 - x_2 - L + a) + \xi_1(t), \\ \dot{x}_2^{(L-a)} &= -\frac{\partial V(x_2)}{\partial x_2} + k(x_1 - x_2 - L + a) + \xi_2(t).\end{aligned}\quad (16)$$

By inserting $x_{11} = x_1 - L$ into Eqs.(16), we have

$$\begin{aligned}\dot{x}_{11}^{(L-a)} &= -\frac{\partial V(x_{11})}{\partial x_{11}} - k(x_{11} - x_2 + a) + \xi_1(t), \\ \dot{x}_2^{(L-a)} &= -\frac{\partial V(x_2)}{\partial x_2} + k(x_{11} - x_2 + a) + \xi_2(t).\end{aligned}\quad (17)$$

By further transforming Eqs.(17) by first $x_{11} \rightarrow x_1$ and then $x_1 \leftrightarrow x_2$, one obtains from Eqs.(17)

$$\begin{aligned}\dot{x}_2^{(L-a)} &= -\frac{\partial V(x_2)}{\partial x_2} + k(x_1 - x_2 - a) + \xi_1(t), \\ \dot{x}_1^{(L-a)} &= -\frac{\partial V(x_1)}{\partial x_1} - k(x_1 - x_2 - a) + \xi_2(t).\end{aligned}\quad (18)$$

Taking into account the same statistical properties of ξ_1 and ξ_2 we finally obtain that

$$\begin{aligned}\dot{x}_2^{(L-a)} &= -\frac{\partial V(x_2)}{\partial x_2} + k(x_1 - x_2 - a) + \xi_2(t) \\ &= \dot{x}_2^{(a)}, \\ \dot{x}_1^{(L-a)} &= -\frac{\partial V(x_1)}{\partial x_1} - k(x_1 - x_2 - a) + \xi_1(t) \\ &= \dot{x}_1^{(a)}.\end{aligned}\quad (19)$$

That is to say,

$$\begin{aligned}v^{(L-a)} &= (\dot{x}_1^{(L-a)} + \dot{x}_2^{(L-a)})/2 = v^{(a)} \\ &= (\dot{x}_1^{(a)} + \dot{x}_2^{(a)})/2,\end{aligned}\quad (20)$$

This interprets the symmetry property of the average velocity against the coupling free length a , shown in Fig.3.

C. Current reversal induced by the potential symmetry coefficient

In studies of Brownian ratchets, the asymmetry coefficient Δ of the potential $V(x)$ plays a significant role in influencing the directional current. In the above discussions we observe the reversal of directed motion by modulating the coupling strength k and the coupling free length a . In fact, the direction can also be determined by the asymmetric coefficient Δ with given a and k . In Fig.5(a), the average velocity against the asymmetric coefficient Δ is plotted for $(k, \Delta\theta) = (1, 0)$, $(300, 0)$ and $(300, \pi)$, respectively, and the other parameters are $t_0=0.1$, $a=0.3$.

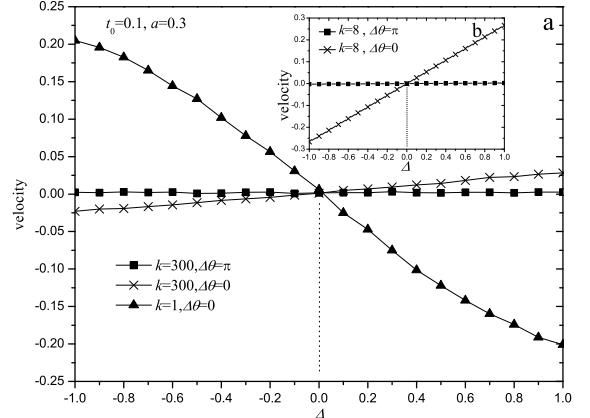


FIG. 5: the average velocity varying with the asymmetric coefficient of $V(x)$.

In the weak-coupling case (e.g., $k = 1$), it can be found from the curve for $k = 1, \Delta\theta = 0$ in Fig.5(a) that $v > 0$ when $\Delta < 0$, $v < 0$ when $\Delta > 0$, and $v = 0$ when $\Delta = 0$. That means the size and the direction of the average velocity is determined by the asymmetric coefficient Δ in this case. In addition, the average velocity decreases approximately linearly with increasing the asymmetric efficient Δ . According to the above analysis, the motion of coupled Brownian motors can be approximately considered as the motion of a single Brownian motor immersed in the periodic potential $V(x)$ and Gaussian white noise when the coupling strength k is small, where the direction of velocity is determined by Δ in the temperature

ratchet model of a single particle. In the strong-coupling case (e.g., $k = 300$), the average velocity, the size and direction of which is also determined by the asymmetric coefficient Δ , linearly increases with increasing the asymmetric coefficient. The curves of the average velocity exhibit a reversed tendency as compared that of the weak-coupling case (e.g., $k = 1$). Moreover, the average velocity for $\Delta\theta = 0$ is larger than that for $\Delta\theta = \pi$ when $k = 300$. Similarly, Fig.5(b) gives the theoretical curve of the average velocity varying with the asymmetric coefficient Δ according to Eq.(10), which qualitatively agrees with simulation results shown in Fig.5(a).

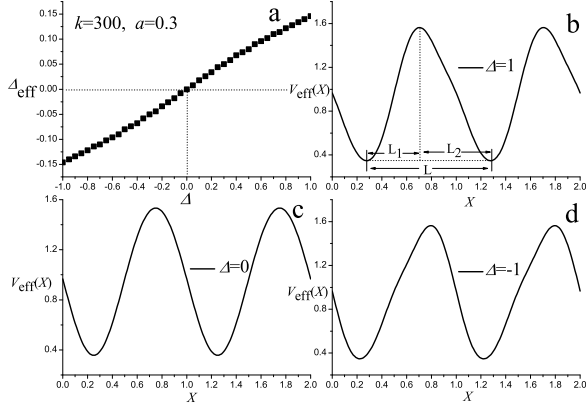


FIG. 6: the effective potential with different asymmetric coefficient.

The effects of asymmetric coefficient Δ on the average velocity can be explained by the effective potential theory for strong coupling case. We introduce an effective asymmetric coefficient Δ_{eff} of the effective potential $V_{eff}(X)$ with the effective asymmetric coefficient $\Delta_{eff} = (L2 - L1)/L$ which is shown in Fig.6(b). When $\Delta_{eff} > 0$ the average velocity $v > 0$ and when $\Delta_{eff} < 0$ the velocity $v < 0$ according to the dynamical mechanism of the temperature-ratchet model. The curve of the effective asymmetric coefficient Δ_{eff} varying with the asymmetric coefficient Δ is plotted in Fig.6(a). One can easily find that the effective asymmetric coefficient linearly increases with the asymmetric coefficient Δ , and when $\Delta = 0$ the effective asymmetric coefficient Δ_{eff} is also zero. Fig.6 (b), (c), (d) shows the effective potential with different asymmetric coefficient Δ given in the plot. It can be seen from Fig.6 that the asymmetry of $V_{eff}(X)$ when $\Delta < 0$ is opposite to that of $\Delta > 0$, and the effective potential $V_{eff}(X)$ is symmetric when $\Delta = 0$. The asymmetry of the effective potential decreases and is close to symmetric with Δ closes to zero. Those results are in agreement with the dependence of the averaged velocity on the asymmetric coefficient Δ for the strong coupling case shown in Fig.5(a).

Moreover, It is noteworthy that every curve in Fig.5(a) is anti-symmetric about $\Delta = 0$ for different coupling

cases. This can be well explained through the analysis of the space-time transformation invariance. In the same way, we rewrite Eq.(1) with a superscript corresponding to the value of asymmetric efficient Δ , and obtain

$$\begin{aligned}\dot{x}_1^{(\Delta)} &= -\frac{\partial V(x_1, \Delta)}{\partial x_1} - k(x_1 - x_2 - a) + \xi_1(t), \\ \dot{x}_2^{(\Delta)} &= -\frac{\partial V(x_2, \Delta)}{\partial x_2} + k(x_1 - x_2 - a) + \xi_2(t).\end{aligned}\quad (21)$$

Adding the two formulas (21), one naturally gets

$$\begin{aligned}\dot{x}_1^{(\Delta)} + \dot{x}_2^{(\Delta)} &= -\left[\frac{\partial V(x_1, \Delta)}{\partial x_1} + \frac{\partial V(x_2, \Delta)}{\partial x_2}\right] \\ &+ \xi_1(t) + \xi_2(t).\end{aligned}\quad (22)$$

By replacing the free length Δ by $L - \Delta$, we have

$$\begin{aligned}\dot{x}_1^{(-\Delta)} + \dot{x}_2^{(-\Delta)} &= -\left[\frac{\partial V(x_1, -\Delta)}{\partial x_1} + \frac{\partial V(x_2, -\Delta)}{\partial x_2}\right] \\ &+ \xi_1(t) + \xi_2(t).\end{aligned}\quad (23)$$

then by putting $V(x) = -V_0[\sin(2\pi x/L) + (\Delta/4)\sin(4\pi x/L)]$ into Eq.(23) we obtain

$$\begin{aligned}\dot{x}_1^{(-\Delta)} + \dot{x}_2^{(-\Delta)} &= \frac{2\pi V_0}{L} \left[\cos\left(\frac{2\pi x_1}{L}\right) - \frac{\Delta}{2} \cos\left(\frac{4\pi x_1}{L}\right) \right. \\ &\left. + \cos\left(\frac{2\pi x_2}{L}\right) - \frac{\Delta}{2} \cos\left(\frac{4\pi x_2}{L}\right) \right] + \xi_1(t) + \xi_2(t),\end{aligned}\quad (24)$$

$$\begin{aligned}\dot{x}_1^{(-\Delta)} + \dot{x}_2^{(-\Delta)} &= -\frac{2\pi V_0}{L} \left[\cos\left(\frac{2\pi x_1}{L} - \pi\right) + \frac{\Delta}{2} \cos\left(\frac{4\pi x_1}{L}\right) \right. \\ &\left. + \cos\left(\frac{2\pi x_2}{L} - \pi\right) + \frac{\Delta}{2} \cos\left(\frac{4\pi x_2}{L}\right) \right] + \xi_1(t) + \xi_2(t).\end{aligned}\quad (25)$$

By further inserting $x_1 = x_{11} + L/2$ and $x_2 = x_{21} + L/2$ into Eq.(25), one has

$$\begin{aligned}\dot{x}_1^{(-\Delta)} + \dot{x}_2^{(-\Delta)} &= -\frac{2\pi V_0}{L} \left[\cos\left(\frac{2\pi x_{11}}{L}\right) + \frac{\Delta}{2} \cos\left(\frac{4\pi x_{11}}{L}\right) \right. \\ &\left. + \cos\left(\frac{2\pi x_{21}}{L}\right) + \frac{\Delta}{2} \cos\left(\frac{4\pi x_{21}}{L}\right) \right] + \xi_1(t) + \xi_2(t).\end{aligned}\quad (26)$$

By further replacing $x_{11} \rightarrow x_1$ and $x_{21} \rightarrow x_2$, it can be found that

$$\begin{aligned}\dot{x}_1^{(-\Delta)} + \dot{x}_2^{(-\Delta)} &= -\frac{2\pi V_0}{L} \left[\cos\left(\frac{2\pi x_1}{L}\right) + \frac{\Delta}{2} \cos\left(\frac{4\pi x_1}{L}\right) \right. \\ &\left. + \cos\left(\frac{2\pi x_2}{L}\right) + \frac{\Delta}{2} \cos\left(\frac{4\pi x_2}{L}\right) \right] + \xi_1(t) + \xi_2(t) \\ &= \left[\frac{\partial V(x_1, \Delta)}{\partial x_1} + \frac{\partial V(x_2, \Delta)}{\partial x_2} \right] + \xi_1(t) + \xi_2(t) \\ &= -(\dot{x}_1^{(\Delta)} + \dot{x}_2^{(\Delta)})\end{aligned}\quad (27)$$

Taking into account the same statistical properties of Gaussian white noises ξ_1 and ξ_2 , and comparing with Eq.(22), eventually we obtain that

$$\begin{aligned} v^{(-\Delta)} &= (\dot{x}_1^{(-\Delta)} + \dot{x}_2^{(-\Delta)})/2 = -(\dot{x}_1^{(\Delta)} + \dot{x}_2^{(\Delta)})/2 \\ &= -v^{(\Delta)} \end{aligned} \quad (28)$$

This implies that the relation between the velocity of the coupled Brownian motors and the asymmetric coefficient Δ obeys an anti-symmetric property. For the special value $\Delta = 0$, this leads to an unbiased motion of the coupled motors, and one has $v^{(0)} = 0$. These results agree well with the effective-potential analysis.

IV. OPTIMIZATION AND MANIPULATION OF COLLECTIVE DIRECTED TRANSPORT

It is interesting to investigate the dependence of directed transport of the system on the coupling strength k and the phase shift $\Delta\theta$ between two motor heads. In this section, we systematically analyze how to optimize the motor motion by modulating the pulsating period and phase shift.

A. Dependence on the pulsating period of temperature

The mean velocity of the coupled motors against t_0 is plotted in Fig.7 for different coupling strengths k and phase shifts $\Delta\theta$ with $\Delta = 1$ and $a = 0.3$. It can be found that the averaged velocity is negative when k is small (e.g., $k = 1$) while the direction of motion is reversed when the coupling strength k is large (e.g., $k = 300$). These results are consistent with the discussion in terms of the effective potential analysis shown in Fig.2b. For the two curves with $k = 300$ the mean velocity is larger for the phase shift $\Delta\theta = 0$ than that for $\Delta\theta = \pi$, and the velocity is nearly zero for the latter.

In Fig.7 we plot the mean velocity as the function of the pulsating period t_0 of the temperature T . It can be clearly seen that all curves of the mean velocity have an optimal pulsating period t_{max} possessing the largest velocity, and the averaged velocity approaches zero when t_0 tends to zero and infinity. This interesting behavior can be interpreted as follows. An infinitely large pulsating period t_0 means that the temperature pulsation is so slow that the temperature can be regarded as a constant. In this case, the coupled Brownian motors is immersed in a stationary periodic potential and a white Gaussian noise with a constant intensity, where the system has a null directed current no matter what the coupling strength k is. On the contrary, when t_0 tends to zero the temperature fluctuations is too fast, and the change of the configuration of coupled Brownian motors always lags behind the rapid temperature fluctuation. This also leads to an absence of directed motion. Moreover, the solid curve

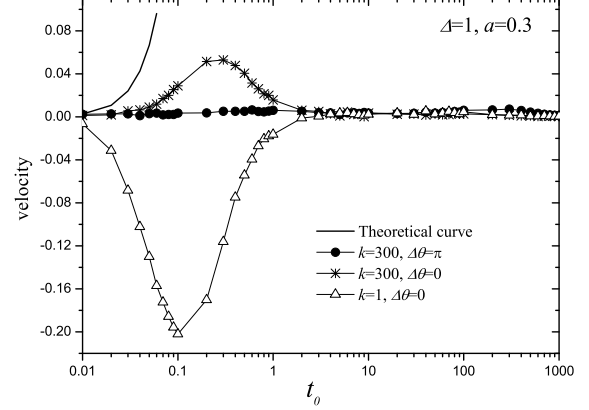


FIG. 7: the mean velocity as the function of the pulsating period t_0 of the temperature T .

in Fig.7 gives the theoretical result according to formula (10) with t_0 and k tending to zero and infinity, respectively. The theoretical results agree well with that of the simulation when t_0 is closed to zero.

B. Dependence on the phase shift between two temperatures

The phase shift $\Delta\theta$ between the temperatures on two motors plays a significant role in influencing the current. In Fig.8(a), the average velocity versus the phase shift $\Delta\theta$ is plotted for the coupling strength $k=1$ and 300, respectively, and other parameters $\Delta=1$, $a=0.3$, and $t_0=0.1$. For very small coupling strength k (e.g., $k=1$), the effect of the phase shift $\Delta\theta$ on the average velocity is almost negligible, where the velocity is approximately a negative constant $v = -0.2$. For the strong couplings (e.g., $k=300$), the phase shift $\Delta\theta$ has important effects on the average velocity, which is clearly shown in Fig.8 for the curve with $k=300$. Moreover, the average velocity varying against the phase shift $\Delta\theta$ is symmetric about $\Delta\theta = \pi$ due to the temporal periodicity of the temperature $T(t)$ about 2π , where v first decreases and then increase with the increase of the phase shift $\Delta\theta$ in the range of 0 to 2π . Fig.8(b) exhibits the theoretical average velocity varying against the phase shift $\Delta\theta$ according to Eq.(10) with the parameters given in the figure, which qualitatively agrees with simulated data shown in Fig.8(a).

V. CONCLUDING REMARKS

To summarize, in this paper we studied the mechanism of collaborated directed transport of elastically coupled Brownian motors in an asymmetric periodic potential un-

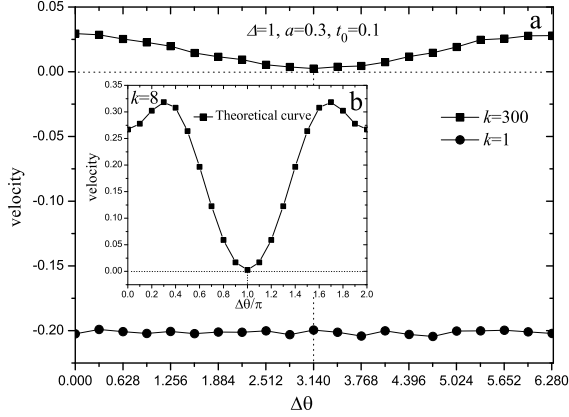


FIG. 8: The average velocity versus the phase difference $\Delta\theta$ with different the coupling strengths k .

der the modulation of two reservoirs with different and asynchronous temperatures. We applied both the invariance analysis of space-time transformation of coupled dy-

namical equations and the effective potential theory to study the coupling-induced symmetry breaking and its consequent collective directed transport and the current reversal behavior. The dynamical analysis indicates that $\Delta \neq 0$ is the precondition of directed motion of the coupled system in this dynamical model, and the presence of the coupling between two motors influences the symmetric breaking of the ratchet system. In the strong-coupling case the directional transport of coupled motors can be reversed by modulating the coupling strength, the coupling free length, or the asymmetry coefficient, which can be effectively illustrated on the basis of the effective potential theory and the invariance analysis of space-time transformation. Moreover, the relations between the average velocity and various parameters are investigated systematically, such as the pulsating period, the phase shift between the temperatures of two reservoirs, and these results provide a valuable way in optimizing and manipulating the collective directed transport by adjusting different parameters in practice.

This work is partially supported by the National Natural Science Foundation of China (Grant Nos.11075016 and 11475022) and the Scientific Research Funds of Huaqiao University.

-
- [1] P. Reimann, M. Evstigneev, Europhys. Lett. **78**, 50004 (2007).
 - [2] F. Marchesoni, Phys. Rev. E **56**, 2497 (1997).
 - [3] J. D. Bao, Y. Z. Zhuo, Chin. Sci. Bull. **43**, 1497 (1998).
 - [4] P. Reimann, Phys. Rep. **361**, 57 (2002).
 - [5] O. M. Braun, R. Ferrando, and G. E. Tommei, Phys. Rev. E **68**, 051101 (2003).
 - [6] S. Goncalves, C. Fusco, A. R. Bishop, and V. M. Kenkre, Phys. Rev. B **72**, 195418 (2005).
 - [7] E. Heinsalu, M. Patriarca, and F. Marchesoni, Phys. Rev. E **77**, 021129 (2008).
 - [8] A. E. Filippov, J. Klafter, and M. Urbakh, Phys. Rev. Lett. **92**, 135503 (2004).
 - [9] S. Maier, Y. Sang, T. Filletter, M. Grant, R. Bennewitz, E. Gnecco, and E. Meyer, Phys. Rev. B **72**, 245418 (2005).
 - [10] H. Y. Wang and J.D. Bao, Phys. A **374**, 33 (2007).
 - [11] J. L. Mateos, Phys. A **351**, 79 (2005).
 - [12] S. E. Mangioni and H. S. Wio, Eur. Phys. J. B **61**, 67 (2008).
 - [13] E. M. Craig, M. J. Zuckermann, and H. Linke, Phys. Rev. E **73**, 051106 (2006).
 - [14] J. Menche and L. Schimansky-Geier, Phys. Lett. A **359**, 90 (2006).
 - [15] M. Evstigneev, S. V. Gehlen, and P. Reimann, Phys. Rev. E **79**, 011116(2009).
 - [16] C. Lutz, M. Reichert, H. Stark, and C. Bechinger, Europhys.Lett. **74**, 719 (2006).
 - [17] T. F. Gao, B. Q. Ai, Z. G. Zheng, and J. C. Chen, Jour. Stat. Mech. **09**, 093204 (2016).
 - [18] H. Y. Wang, J. D. Bao, Phys. A **389**, 433 (2010).
 - [19] Z. G. Zheng, Commun. Theor. Phys. **43**, 1072 (2005).
 - [20] B. O. Yan, R. M. Miura, Y. D. Chen, J. Theor. Bio. **210**, 141(2001).
 - [21] A. Pototsky, N.B. Janson, F. Marchesoni, and S. Savelev, Europhys. Lett. **88**, 30003 (2009).
 - [22] Z. G. Zheng, G. Hu, B. Hu, Phys. Rev. Lett. **86**, 2273 (2001).
 - [23] S.V. Gehlen, M. Evstigneev, and P. Reimann, Phys.Rev.E **79**, 031114 (2009).
 - [24] H. Y. Wang, J. D. Bao, Phys. A **337**, 13 (2004).
 - [25] Z. G. Zheng, M. C. Cross, G. Hu, Phys. Rev. Lett. **89**, 157102 (2002).
 - [26] Z. G. Zheng, H. B. Chen, Europhys. Lett. **92**, 3004 (2010).
 - [27] S.V. Gehlen, M. Evstigneev, and P. Reimann, Phys. Rev. E **77**, 031136 (2008).
 - [28] A. D. Rogat, K. G. Miler, J. Cell Sci. **115**, 4855 (2002).
 - [29] H. Park, A. Li, L. Q. Chen, A. Houdusse, P. R. Selvin, H. L. Sweeney, Proc. Acad. Sci. **104**, 778 (2007).
 - [30] E. M. Delacruz, E. M. Ostap, H. L. Sweeney, J. Bio. Chem. **276**, 32373 (2001).
 - [31] S. Nishikawa, K. Homma, Y. Komori, M.Iwaki, T. Wazawa, A.H. Iwone, J.Saito, R. Ikebe, E. Katayama, T.Yanagida, M.Ikebe, Biochem. Biophys. Res. Commun. **290**, 311 (2002).
 - [32] A. Wunderlin, H. Haken, Zeitschrift fr Physik B Condensed Matter **44**, 135 (1981).
 - [33] J. C. Chen, G. Z. Su, *Thermodynamics and statistical physics (Vol.1)* (Science Press, Beijing, 2010)(in Chinese).
 - [34] J. D. Bao, *Stochastic simulation method of classical and quantum dissipative systems* (Science Press, Beijing, 2009)(in Chinese).
 - [35] Z. G. Zheng, *Collective behaviors and spatiotemporal dynamics in coupled nonlinear system* (Higher Education

Press, Beijing, 2004)(in Chinese).

- [36] H. B. Chen, Q.W. Wang, Z. G. Zheng, Phys. Rev. E **71**, 031102 (2005).